# Relation between Charge Transfer Absorption and Fluorescence Spectra and the **Inverted Region**

#### R. A. Marcus

Noves Laboratory of Chemical Physics, California Institute of Technology, Pasadena, California 91125 (Received: August 22, 1988; In Final Form: October 7, 1988)

The theoretical expression for the plot of a charge transfer (CT) band intensity vs frequency is known to parallel that for the plot of electron-transfer rate constant  $k^{ET}$  vs  $-\Delta G^0$ . We use this parallelism to explore a recent model in the literature on the possible role, if any, of partial dielectric saturation of the solvent on the "inverted region" of electron-transfer reactions. A simple approximate expression is obtained for the full width at half-maximum for the  $k^{\rm ET}$  and spectral plots and is tested using recent numerical results for calculated  $k^{ET}$  vs  $-\Delta G^0$  curves. Studies of experimental widths of CT bands are used, thereby, to test ideas on the possible presence and effects of partial dielectric saturation and on the observation of the inverted region. Further uses of charge-transfer spectra, when both the absorption and fluorescence data are available, are also described, including the determination of the "0  $\rightarrow$  0 transition energy"  $\Delta E_{0\rightarrow0}$  for systems displaying little or no vibrational structure.

#### Introduction

Electron-transfer processes may arise thermally or, as reflected in charge-transfer spectra, from the absorption or emission of light. It is well-known that there is a close relationship between the two. 1-4 In the present paper this relationship is utilized to study a recent interesting suggestion of Kakitani and Mataga<sup>5</sup> concerning a possible dielectric saturation effect in the vicinity of an organic ion, and its role in the observability of the inverted effect. The "inverted region", it will be recalled,6 is a region where the electron-transfer rate constant  $k^{ET}$  decreases, instead of increases, with increasingly negative standard free energy of reaction  $\Delta G^0$ in a series of similar reactions. It was postulated<sup>5</sup> that in a charge separation reaction, where two neutral reactants yield two ions as a result of an electron transfer, a partial dielectric saturation occurs and would inhibit or largly inhibit the observation of the inverted effect, but would accentuate it in the reverse reaction of charge recombination.5

We first compare the treatment of charge-transfer spectra with that for a rate constant of a thermal electron transfer reaction. In the former the data involve a plot of a (reduced) absorbance or fluorescence intensity vs  $h\nu$ , while in the latter the plot is one of the rate constant  $k^{\rm ET}$  vs  $-\Delta G^0$ . The very existence of the well-known maximum in the former corresponds, as we have pointed out earlier,  $^{3b}$  to the  $k^{\rm ET}$  passing through a maximum in the latter, and thereby to the phenomenon known as the inverted effect.

Next, a simple approximate expression is obtained for W, the full width at half-maximum for these two plots. To explain the apparent absence of an inverted region in various fluorescence quenching charge separation reactions, parameters<sup>7</sup> were introduced in ref 5 which, in effect, led to a very large predicted W for those reactions. We test the present simple expression for W by comparing with values for W found from the detailed numerical calculations  $^{5a}$  for the  $k^{\rm ET}$  vs  $-\Delta G^0$  plots. The present results are then applied to a variety of data on charge-transfer spectra, and suggestions are made regarding future experiments and the interpretation of existing ones.

Also given are several other results, including a method for determining the "0  $\rightarrow$  0 transition energy"  $\Delta E_{0\rightarrow 0}$  for systems displaying little or no vibrational structure. Both the case where the mirror-image absorption-fluorescence rule prevails and the case when deviations occur due to unequal force constants are treated.

## Theory

We first consider the parallelism of the thermal and optical ET phenomena from a classical point of view, which provides a useful simple physical picture of their relationship. The potential

energy of the two redox reactants (either separated or attached via a molecular bridge) and of the entire surrounding solvent is a function of the many coordinates in the system, N in number. There is such a potential energy function for the reactants  $U^{r}$  and another function for the products  $U^p$ . A profile of these two N + 1 dimensional surfaces along a vibrational coordinate will be rather simple, largely a parabola, but along a solvational coordinate it can be much more complex with many local minima. The two surfaces intersect and their intersection occurs on an N-1 dimensional set of points in coordinate space. If the U<sup>p</sup> surface is raised or lowered vertically with respect to the  $U^{\tau}$  surface, the intersection occurs at a different value of the remaining (Nth) coordinate q. Using such successive vertical displacements, the corresponding successive intersections define successive values of  $q^{6,8}$  In thermal electron transfers the intersection of the  $U^{\dagger}$  and  $\dot{U}^p$  surfaces,  $U^r - U^p = 0$ , defines the position of the transition state in N-dimensional coordinate space, for the given  $\Delta G^{0.6,8}$ 

The thermal electron transfer rate constant  $k_{rp}^{ET}$  for the reaction  $r \rightarrow p$  is, using transition-state theory, proportional to the integral  $\int ... \int \exp(-U^{r}/k_{\rm B}T) dq_1 ... dq_{N-1}$ , if the dependence of the electron-transfer matrix element on coordinates is neglected (Condon approximation).<sup>6,8</sup> (The coordinate  $q_N$  is the coordinate q described above.) This integral over  $dq_1 \dots dq_{N-1}$  can be written as  $\exp(-G^{r}(q)/k_{B}T)$ , where  $G^{r}(q)$  is the configurational free energy of a system in the electronic state r, constrained to lie on this N-1 dimensional set of coordinates at the specified q. A plot of  $G^{r}(q)$  and of  $G^{p}(q)$  is relatively simple, in contrast to the many-dimensional  $U^{p}(q_{1}...q_{N})$  and  $U^{p}(q_{1}...q_{N})$  surfaces. It is depicted in Figure 1a for a thermal electron transfer reaction. (In the dielectric unsaturation approximation these plots of G(q) are parabolas.<sup>6,8</sup>) This relationship between free energy G(q) and a many-dimensional potential energy surface is discussed in ref 6, 8, and, more pictorially, 3c.

<sup>&</sup>lt;sup>†</sup>Contribution No. 7825.

<sup>(1)</sup> Marcus, R. A. J. Chem. Phys. 1965, 43, 1261. This article also contains solvent shift expressions for the ellipsoidal model in addition to the dipole in a sphere and the pair of spheres models.
(2) Hush, N. S. Prog. Inorg. Chem. 1967, 8, 391; Electrochim. Acta 1968,

<sup>13, 1005.</sup> These references are the classic references to intervalence spectra. (3) (a) Ulstrup, J.; Jortner, J. J. Chem. Phys. 1975, 63, 4358. Jortner, J. Ibid. 1976, 64, 4860. (b) Siders, P.; Marcus, R. A. J. Phys. Chem. 1982, 86, 622. (c) Marcus, R. A.; Sutin, N. Comments Inorg. Chim. 1986, 5, 119. In

<sup>(</sup>a) and (b) the relationship between the two types of processes, although discussed, is largely "buried" in a discussion of other aspects.
(4) E.g.: Piepho, S. B.; Krausz, E. R.; Schatz, P. W. J. Am. Chem. Soc. 1978, 100, 2996. Bukhs, E. Ph.D. Thesis, Tel-Aviv University, 1980. Redi, M.; Hopfield, J. J. Chem. Phys. 1980, 72, 6651.
(5) (a) Kakitani, T.; Mataga, N. J. Phys. Chem. 1987, 91, 6277.
(b) Kakitani, T.; Mataga, N. Ibid. 1986, 90, 993.
(c) Kakitani, T.; Mataga, N. Phys. Chem. Light in (a) Mataga, N. Phys. Lett. 1986, 124, 427, and other available in (b) Mataga, N.

Chem. Phys. Lett. 1986, 124, 437, and other articles cited in (a).

<sup>(6)</sup> Marcus, R. A. Discuss. Faraday Soc. 1960, 29, 21. (7) E.g., a value of  $\beta = 0.1$  in the notation of ref 5, used in a fit there to

some of the data, corresponds to a ratio of  $k_p/k_r = 11$ , in the present notation. (8) Marcus, R. A. J. Chem. Phys. 1965, 43, 679.



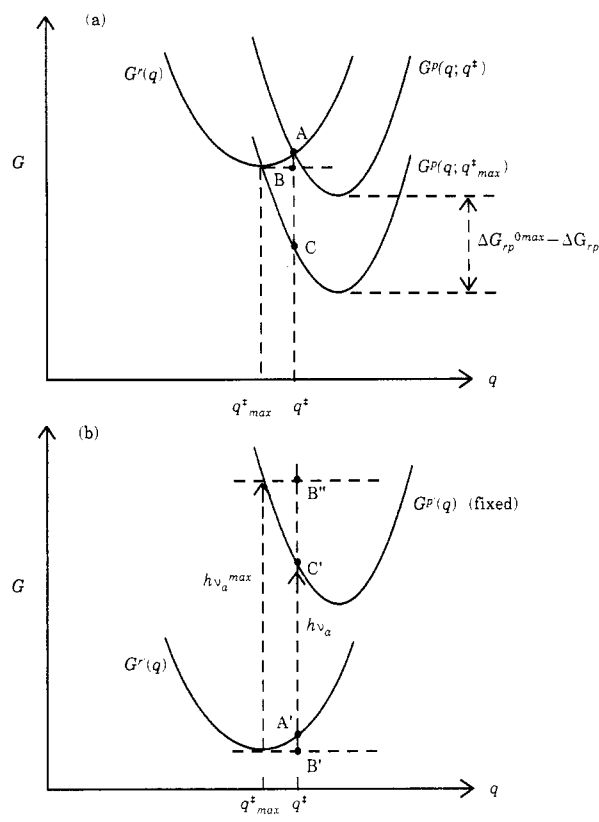


Figure 1. Plot of free energies G for the r and p electronic states vs the coordinate q defined in the text. (a) Thermal electron transfer reaction, with plots for two different values of  $\Delta G^0_{rp}$  indicated; (b) optical transition, with two different absorption frequencies indicated.

If this  $U^{\tau}$  surface is lowered vertically by an amount  $\Delta E$ , we now have  $U^p = U^r + \Delta E$  at the above value of q. Based on the Franck-Condon principle, the absorption of a light quantum  $h\nu$ =  $\Delta E$  occurs ony for this same N-1 dimensional set of points represented by this particular value of q (Figure 1b). The absorbance between  $h\nu$  and  $h\nu + h d\nu$  arises from systems lying between q and q + dq and so is proportional to  $h d\nu (dq/h d\nu)$  $\int ... \int \exp(-U^r/k_B T) dq_1 ... dq_{N-1}$  and, thereby, to  $\exp(-G^r(q)/k_B T)$ , when the dependence of the dipole matrix element for the optical absorption on coordinates is neglected. The quantitative parallelism of the two phenomena is thus clear, as indeed has been seen in various ways in previous work.1-4

To any particular value of the vertical displacement of the  $U^p$ surface relative to the  $U^{\tau}$  surface there corresponds a particular value of  $\Delta G^0_{rp}$ , the standard free energy for the reaction  $r \rightarrow p$ . If the  $U^p$  surface is lowered vertically by some amount,  $\Delta G^0_{rp}$  is thereby made more negative by exactly that amount, since this vertical shift has no effect on the distribution of coordinates and momenta on the  $U^{r}$  surface or on the  $U^{p}$  surface: It has therefore no effect on the standard entropy change  $\Delta S^0$  and on the average thermal energy (potential and kinetic) change during the reaction. The value of  $\Delta G^0$  which produces the maximum thermal ET rate constant  $k_{\rm rp}^{\rm ET,max}$  is denoted by  $\Delta G^{\rm 0 \, max}$ . The corresponding  $G^{\rm p}$ curve in Figure 1a is labeled  $G^{p}(q;q^{*}_{max})$  and intersects the minimum of the  $G^{r}(q)$  curve (no free energy barrier). The q at this intersection is denoted in Figure 1a by  $q^*_{\text{max}}$ . At some other  $\Delta G_{\rm rp}^0$ , producing a curve  $G^{\rm p}(q;q^*)$ , the intersection occurs at some other  $q^*$ . We have, for this situation of weak electronic coupling of the r and p states

$$k_{\rm rp}^{\rm ET}/k_{\rm rp}^{\rm ET,max} = e^{-\Delta G^{\dagger}_{\rm rp}(q^{\dagger})/k_{\rm B}T}$$
 (1)

where  $\Delta G_{\rm rp}^{\ \dagger}(q^{\ \dagger})$  is the vertical distance BA in Figure 1a. We turn next to the absorbance. The  $G^{\rm r}$  curve in Figure 1b is the same as that in Figure 1a but shifted vertically downward so as to permit light absorption (a charge-transfer absorption) instead of the thermal charge transfer reaction described in Figure 1a. Associated with the absorbance  $\epsilon_{\nu}$  at the indicated absorption frequency  $\nu_{\rm a}(q^{\rm *})$  is the probability factor  $\exp[-\Delta G^{\rm *}_{\rm rp}(q^{\rm *})/k_{\rm B}T]$ discussed earlier. This  $\Delta G^{*}_{p}(q^{*})$  equals the vertical distance B'A' in Figure 1b. We have, thereby, for this case of weak electronic coupling of the r and p states

$$(\epsilon_{\nu}/\nu)/(\epsilon_{\nu}/\nu)_{\text{max}} = e^{-\Delta G^{\bullet}_{\text{rp}}(q^{\bullet})/k_{\text{B}}T}$$
 (2)

where the  $1/\nu$  occurs as part of the standard electromagnetic expression<sup>9,10</sup> given later. The B'A' in Figure 1b equals the BA in Figure 1a. The maximum absorbance  $\epsilon_{\nu}^{\text{max}}$  occurs at a  $\nu_a$  =  $v_a^{\text{max}}$ , corresponding to a  $q^* = q^*_{\text{max}}$  depicted in Figure 1b. We thus have from (1) and (2):

$$k_{\rm rp}^{\rm ET}/k_{\rm rp}^{\rm ET,max} = (\epsilon_{\nu}/\nu)/(\epsilon_{\nu}/\nu)_{\rm max}$$
 (3)

We turn next to the relationship between the  $\Delta G^0_{rp}$  and  $\Delta G^0_{rp}^{max}$  of Figure 1a and the  $h\nu_a$  and  $h\nu_a^{max}$  of Figure 1b. The difference of  $\Delta G^0_{rp}$ 's in Figure 1a, namely,  $\Delta G^0_{rp}^{max} - \Delta G^0_{rp}$ , can be seen there accordingly  $\Delta G^0_{rp}^{max} = \Delta G^0_{rp}^{max}$ . to equal CA in magnitude, which in turn equals CB + BA, and the latter, in turn, equals the C'B" + B'A' in Figure 1b. This sum equals the  $h\nu_a^{\text{max}} - h\nu_a$ . Thereby, we have

$$\Delta G^{0}_{rp} = \Delta G^{0}_{rp}^{\text{max}} + h\nu_{a}^{\text{max}} - h\nu_{a}$$
 (4)

Similarly, for the fluorescence emission intensity  $f_{\nu}$  we have

$$(f_{\nu}/(\nu^3))(f_{\nu}/(\nu^3)_{\text{max}}) = k_{\text{pr}}^{\text{ET}}/k_{\text{pr}}^{\text{ET,max}}$$
 (5)

the  $\nu^3$  occurring as part of the standard electromagnetic expression.<sup>9,10</sup> Corresponding to (4) we have

$$\Delta G^0_{\text{pr}} = \Delta G^0_{\text{pr}}^{\text{max}} + h \nu_{\text{f}}^{\text{max}} - h \nu_{\text{f}} \tag{6}$$

where  $\Delta G^0_{
m pr}^{
m max}$  and  $u_{
m f}^{
m max}$  are the  $\Delta G^0_{
m pr}$  and  $u_{
m f}$  at which  $k_{
m pr}^{
m ET}$  and  $f_{\nu}/\nu^3$  have their maxima.

Thus, a plot of  $k^{\rm ET}$  vs  $\Delta G^0$  corresponds to a plot of  $\epsilon_{\nu}/\nu$  [(3) and (4)] or to  $f_{\nu}/\nu^3$  [(5) and (6)] vs  $h\nu$ . The well-known existence of a maximum in these two charge-transfer spectra corresponds to the existence of a maximum in the rate constant plots. As can be seen from (3) and (4), the decrease of  $\epsilon_{\nu}/\nu$  with increasing  $\nu$ on the high-frequency side of the charge transfer absorption maximum corresponds to the decrease of  $k_{rp}^{ET}$  with increasingly negative  $\Delta G^0$ , i.e., to the inverted region for the  $r \rightarrow p$  electrontransfer reaction. Similarly, on the low-frequency side of the charge transfer fluorescence maximum the decrease of  $f_{\nu}/\nu^3$  with decreasing  $\nu$  corresponds to (5) and (6) to the decrease of the electron-transfer rate constant  $k_{\rm pr}^{\rm ET}$  with increasingly negative  $\Delta G^0_{\rm pr}$ , i.e., to the "inverted region" for the p  $\rightarrow$  r reaction. We note that the parallelism expressed in (3) and (4) and in (5) and (6) applies regardless of whether the  $G^p$  curve has the same curvature as the  $G^{r}$  one, and, indeed, regardless of whether they are or are not parabolas.

We turn next to the quantum expression. In the Golden rule expression for electron-transfer rate constant<sup>3,11</sup> and that for absorbance<sup>9,10</sup>  $\epsilon_{\nu}/\nu$  or fluorescence<sup>9,10</sup>  $f_{\nu}/\nu^3$  the same one-to-one parallelism3 between the two (considered more fully in a later section) is seen when the Condon approximation is introduced, i.e., when the dependence of the respective optical dipole and electron-transfer matrix elements on coordinates is neglected. The same conclusion again follows, namely, that the high-frequency side of the charge transfer absorption band and the low-frequency side of the CT fluorescence band each correspond to the inverted region in thermal electron transfer reactions. We also note that any mirror-image behavior in the absorption/fluorescence spectra thus reflects a corresponding mirror-image behavior of plots of  $k_{\rm rp}$  and  $k_{\rm pr}$  vs  $\Delta G^0_{\rm rp}$ , and thereby (a significant point) for the

<sup>(9)</sup> Förster, Th. Fluoreszenz Organischer Verbindungen; Vandenhoeck and

Ruppert: Gottingen, 1951; Sections 12 and 26.
(10) Mataga, N.; Kubota, T. Molecular Interactions and Electronic Spectra; Dekker: New York, 1970. We use (3-36)-(3-38) there, p 120, summed over all states, suitably weighted with a Boltzmann factor, to obtain

<sup>(11)</sup> Levich, V. G.; Dogonadze, R. R. Dokl. Chem. Phys. Chem. Sect. (Engl. Transl.), 1959, 124, 9. Levich, V. G.; Dogonadze, R. R. Collect. Czech. Chem. Commun. 1961, 26, 193; Transl., Boshko, O., Ottawa. Levich, V. G. Adv. Electrochem. Electrochem. Eng. 1966, 4, 249.

charge-recombination (CR) and charge-separation (CS) reactions discussed later.

### **Expressions for Absorption and Fluorescence**

We next recall the Golden rule expression for the absorbance  $\epsilon_{\nu}$  for an r  $\rightarrow$  p optical transition. Neglecting the dependence of the optical dipole matrix element on the coordinates we have<sup>9,10</sup> for the molar absorbance  $\epsilon_{\nu}$ , defined by  $-\log I/I_0 = \epsilon_{\nu}ML$ , where M is the molar concentration of the solute,  $I_0$  and I are the incident and transmitted light intensity, and L is the optical path length:

$$\epsilon_{\nu}/\nu = (C_{a}/\delta\nu) \sum_{n,m} |\langle \Psi_{n}^{p} | \Psi_{m}^{r} \rangle|^{2} e^{-E_{n}^{r}/k_{B}T}$$
 (7)

where the sum is over states whose  $r \rightarrow p$  transition energies lie in a narrow range of frequencies  $\delta \nu$ :

$$h\nu \le E_m^{\rm p} - E_n^{\rm r} + \Delta E_{\rm rp}^0 \le h(\nu + \delta\nu) \tag{8}$$

 $E_m^p$  and  $E_n^r$  denote the *m*th and *n*th energy levels of the p and r electronic states, respectively, each measured relative to its lowest state for the nuclear motion. The wave functions for the nuclear motion on the p and r surfaces are denoted in (7) by  $\Psi_m^p$  and  $\Psi_n^r$ .  $\Delta E^0_{rp}$  is the  $0 \to 0$  transition frequency, i.e., the energy of the lowest state of the p electronic state minus that of the r state. In (7)  $C_a$  is given by

$$C_a = 8\pi^3 N_A' |\mu_{rp}|^2 / (3hncQ_r \ln 10)$$

where  $N_{\rm a}{}'$ ,  $\mu_{\rm rp}$ , n, c, and  $Q_{\rm r}$  denote Avogadro's number divided by  $10^3$ , the square of the electronic factor in the transition dipole matrix element for the r  $\rightarrow$  p transition, the refractive index of the medium, the velocity of light, and the partition function of the system when the solute is in the r electronic state.

Similarly, for the fluorescence spectrum for the p  $\rightarrow$  r transition the probability of emission of a photon per unit time in the frequency range  $(\nu, \nu + \delta \nu)$  is  $f_{\nu} \delta \nu$ , where  $^{9,10}$ 

$$f_{\nu}/\nu^{3} = (C_{\rm f}/\delta\nu) \sum_{n,m} |\langle \Psi_{n}^{\ r} | \Psi_{m}^{\ p} \rangle|^{2} e^{-E_{m}^{\ p}/k_{\rm B}T}$$
 (10)

The sum in (10) is over states m and n satisfying (8), and  $C_f$  is given by

$$C_{\rm f} = 64\pi^4 n |\mu_{\rm rp}|^2 / ehc^3 Q_{\rm p} \tag{11}$$

where  $Q_{\rm p}$  denotes the partition function of the entire system with the solute in the p electronic state. As is customary,  $\epsilon_{\nu}$  is in units of area, and  $f_{\nu}\delta\nu$  in units of reciprocal time. <sup>9,10</sup>

General semiclassical expressions  $^{12}$  are next introduced for the wave functions  $\Psi_m^P$  and  $\Psi_n^T$ , expressions which are applicable to the many nuclear coordinates which are classical-like, including the orientational coordinates of the solvent molecules and any low-frequency vibrations, while any remaining part of the wave function refers to high-frequency vibrations and so is treated quantum mechanically. One feature of the general semiclassical wave functions is that they apply to rotations, hindered rotations, vibrations, etc., and do not presume any separability of these motions, which can be individual or collective in nature. We first consider the case where the statistical mechanical equivalent of a dielectric unsaturation approximation is introduced. Hence, (12)–(15) below are not intended to apply to the Kakitani–Mataga model.  $^5$ 

We adapt the results derived elsewhere for electron-transfer reactions. <sup>12</sup> Namely, the general semiclassical treatment of ref 12 is used for the cited modes, together with the molecular (statistical mechanical) form of dielectric unsaturation approximation. A quantum treatment is retained for any high-frequency modes. To this end we first convert the starting expression in ref 12 to one resembling (7)–(11). Equation 1 of ref 12, after being multiplied by a Boltzmann factor and integrated over a small range of energies  $\delta E$ , can be rewritten (in the notation of ref 12) as

$$k_{\alpha\beta}(T) = \frac{2\pi V^2}{\hbar} \frac{1}{\delta E} \sum_{f} |\langle \Psi_f | \Psi_i \rangle|^2 e^{-E_t/k_B T} / Q_{\rm r}$$
 (12)

where the sum is over the initial and final states i and f for which  $0 \le E_f - E_i + \Delta E^0 \le \delta E$ . (The i of ref 12 denotes the present n for electronic state r, and f denotes the present m for state p.) Comparison with the present (7) and (8) for  $\epsilon_{\nu}$  shows that, apart from notation, the  $2\pi V^2/\hbar$  in (12) is replaced by  $C_a h$  (since  $\delta E = h\delta \nu$ ) and  $\Delta E^0$  is replaced by  $\Delta E^0 - h\nu$ . With this change we can immediately apply (25) of ref 12, yielding<sup>13</sup>

$$\epsilon_{\nu}/\nu = C_{a}h\sum_{n,m}|\langle\phi_{n}^{r}|\phi_{m}^{p}\rangle|^{2}(4\pi\lambda_{0}k_{B}T)^{-1/2}Q_{\nu r}^{-1} \exp[-\{\epsilon_{n}^{r}+(\epsilon_{m}^{p}-\epsilon_{n}^{r}+\Delta G^{0}_{rp}^{s}+\lambda_{0}-h\nu)^{2}\}/4\lambda_{0}k_{B}T]$$
(13)

Similarly for  $f_n$  we have

$$f_{\nu}/\nu^{3} = C_{f} h \sum_{n,m} |\langle \phi_{n}^{r} | \phi_{m}^{p} \rangle|^{2} (4\pi \lambda_{0} k_{B} T)^{-1/2} Q_{vp}^{-1} \exp[-[\epsilon_{m}^{p} + (\epsilon_{n}^{r} - \epsilon_{m}^{p} + \Delta G_{rp}^{0}^{s} + \lambda_{0} + h\nu)^{2}] / 4\lambda_{0} k_{B} T]$$
 (14)

where m and n now refer only to the high-frequency modes. The  $\phi$ 's and energies  $\epsilon$ 's denote any high-frequency vibrational wave functions and their energy levels, respectively, each such  $\epsilon$  being measured relative to the lowest level in that electronic state r or p; the partition function for these modes in the r state is  $Q_{vr}$  and in the p state is  $Q_{vp}$ ;  $\lambda_0$  is the reorganizational parameter for the modes of the solvent and for any other low-frequency modes; and  $\Delta G^0_{rp}$ 's denotes the free energy change for the  $r \to p$  transition, apart from the enthalpy and entropy change due to excitations in the quantized modes. When the vibration frequency of those quantized modes is high, they make a negligible contribution to  $\Delta S^0_{rp}$  and to the thermal energy change (the energy change in excess of the  $0 \to 0$  value), and then  $\Delta G^0_{rp}$ 's becomes  $\Delta G^0_{rp}$ . This is, in fact, the case modeled below. One feature of (13) and (14) is the occurrence of the  $\Delta G^0$ , rather than the  $\Delta E^0$  sometimes seen in related expressions derived under more restrictive assumptions.

The focus in experimental intramolecular or intermolecular charge transfer spectra has almost always been on the positions of the absorption or fluorescence maxima, though occasionally their widths or shapes are discussed, e.g., ref 1-3 and 14. The shapes of the plots, often not treated in detail, can be of particular interest nevertheless, particularly in the currently few cases where both the absorption and fluorescence spectra for the same electronic transition  $r \leftrightarrow p$  are available.

tronic transition  $r \leftrightarrow p$  are available.

Indeed, plots of  $\epsilon_{\nu}/\nu$  and  $f_{\nu}/\nu^3$  vs  $\nu$  play the same role in charge-transfer spectra that  $k^{ET}$  vs  $-\Delta G^0$  plots play in thermal electron transfer reactions. There are some differences of course: The range of values of  $k^{ET}$  in these plots can be enormous, covering many orders of magnitude, while in the spectral plots signal/noise effects and the presence of other bands may interfere. For completeness expressions for the shapes of these plots are given for the dielectrically unsaturated case in the Appendix.

#### Role of Possible Dielectric Saturation

Kakitani and Mataga<sup>5</sup> have considered three different types of electron transfers: a charge-separation reaction (two neutrals  $\rightarrow$  two ions), the reverse reaction of charge recombination, and a charge-shift reaction in which a neutral and a singly charged ion interchange a charge. They suggested that each reaction type should show a different effect of dielectric saturation on the inverted region. (The most common example of a charge-separation reaction is the fluorescence quenching of a neutral reactant by electron transfer with another reactant to form two radical ions.) Expressions were obtained in ref 5a for the  $k^{\rm ET}$  vs  $\Delta G^0$  behavior in all three cases, taking into account the reorganization of several parts of the system during the reaction: a partially dielectrically saturated solvent shell around each reactant (partially

<sup>(13)</sup> This expression has usually been obtained using a harmonic oscillator potential energy formulation (e.g., ref 2). However, it also follows more generally, in the dielectric unsaturation case, from more realistic solute-solvent potential energy surfaces which can, in many-dimensional space, have numerous local minima.

<sup>(14) (</sup>a) Creutz, C. Prog. Inorg. Chem. 1983, 30, 1, and references cited therein. (b) Powers, M. J.; Meyer, T. J. J. Am. Chem. Soc. 1978, 100, 4393. (c) Penfield, K. W. et al., ref 27. (d) Brunschwig, B. S.; Ehrenson, S.; Sutin, N. J. Phys. Chem. 1986, 90, 3657.

TABLE I: Comparison of Simple Expressions for Widths and Maxima with Numerical Results<sup>a</sup>

reaction			W, eV	$-\Delta G^{0 \text{ max}}$ , eV		
type	β	KM	eq 28-30	KM	eq 31-33	
CS	0.1	1.79	1.87	1.64	1.80	
CSH	0.1	1.18	1.38	1.14	1.35	
CR	0.1	0.56	0.56	0.91	0.89	
CS	0.3	1.24	1.21	1.74	1.80	
CSH	0.3	0.95	0.94	1.35	1.42	
CR	0.3	0.57	0.53	1.03	1.03	
CS	<b>∞</b>	0.77	0.77	1.80	1.80	
CSH	œ	0.77	0.77	1.80	1.80	
CR	œ	0.77	0.77	1.80	1.80	

 $^a\hbar\omega$ ,  $\lambda_p$ ,  $\lambda_i$ , and  $\lambda_0$  equal 0.1, 1.0, 0.3, and 0.5 eV, respectively; T=300 K. The ratio  $k_p/k_r$ , and hence  $\lambda_p/\lambda_r$ , is obtained from the value of  $\beta$ :  $k_p/k_r=(1+\beta)/\beta$ . Numerical results labeled KM were obtained from the data provided by T. Kakitani.<sup>20</sup> For  $\beta = \infty$ , i.e.,  $k_p = k_r$ , the dielectrically saturated theory<sup>5</sup> reduces to the unsaturated one.

saturated only when a reactant is charged), the solvent outside of that shell, and (treated quantum mechanically) an intramolecular vibration.5

We explore now the effect of "a partial dielectric saturation" on the charge-transfer spectral properties, using the solvent model postulated in ref 5a for thermal electron transfers. Later in the paper we describe the testing of quantitative implications of that model using CT spectra.

To explain the apparent absence of the inverted effect in charge-separation (CS) reactions of the fluorescence quenching type, a dielectric saturation was introduced and parameters used which led to a very broad  $k^{\rm ET}$  vs  $\Delta G^0$  plot in the vicinity of the maximum of  $k^{\rm ET}$  for CS reactions.<sup>5</sup> For example, near the maximum of that plot a variation of  $k^{\rm ET}$  of roughly only a factor of 2 was calculated in the theory when  $\Delta G^0$  was varied by almost 2 eV for one example of a CS reaction (ref 5a and the present Table I). In the present section we obtain a simple approximate expression, for the model in ref 5a, for the full width at halfmaximum W for these  $k^{\rm ET}$  vs  $\Delta G^0$  plots. Thereby, we also obtain this width for the corresponding charge transfer absorption or fluorescence spectra. The correctness of the partially saturated model is then examined by studying the experimental widths in the CT spectral data. The present expressions are first tested by a comparison with some detailed numerical calculations.5a The resulting agreement, described later, indicates the usefulness of the present simple expressions, which can then be applied to the experimental data.

We first consider the solvent inside the partially saturated shell and the high-frequency vibrations and later include the solvent outside the shell. The model is chosen to be the same as that employed in ref 5a:

If the solvation free energy is plotted vs a generalized solvation fluctuation coordinate x for the two electronic states, the local curvatures, i.e., the "force constants"  $k_p$  and  $k_r$  of these plots, would be equal only if the solvent in this shell were dielectrically unsaturated.<sup>15</sup> However, in ref 5 it was postulated that in the immediate vicinity of an organic ion this force constant for the (first shell) solvent dielectric polarization is much larger than that when the reactant is uncharged (a factor of 11 in some cases).

The solvation free energies  $G_r^s(x)$  and  $G_p^s(x)$  are then written as15,16

$$G_{\rm r}^{\rm s}(x) = \frac{1}{2}k_{\rm r}x^2, \quad G_{\rm p}^{\rm s}(x) = \frac{1}{2}k_{\rm p}(x-a)^2$$
 (15)

where x = 0 and x = a describe the equilibrium configurations of the solvent polarization function parameter x in the r and p states, respectively, and where the G for each electronic state r or p is calculated relative to the equilibrium solvation free energy for that state. (In a detailed calculation<sup>5</sup> two such x-parameters were introduced one per reactant, but for our immediate purpose, in the case of CS and CR reactions, one parameter will suffice. 16)

For any given quantized vibrational states m and n of electronic states p and r, respectively, and for an absorption or fluorescence frequency  $\nu$  the value of x is the solution of the equation

$$h\nu(x) = G_p^{s}(x) - G_r^{s}(x) + m\hbar\omega_p - n\hbar\omega_r + \Delta G_{rp}^{0}$$
 (16)

for the case of a single high-frequency vibrational mode. The spacing of energy levels for this mode is denoted by  $\hbar\omega_r$  and  $\hbar\omega_p$ in the r and p states, respectively. (In ref 5a the approximation  $\omega_{\rm r} = \omega_{\rm p}$  is used.) In (16)  $\Delta G^0_{\rm rp}$  is the electronic (0  $\rightarrow$  0) energy difference of the two states, plus the difference between the equilibrium values of the solvation free energies of the two states. The value of x in (16) clearly depends on both m and n. There is also in ref 5a an additional (unsaturated) solvent contribution which we include later in this paper but omit now for simplicity of presentation. Equation 16 and the final results below [(28)–(33)] are readily extended to the case where there is more than one high-frequency mode.

The absorbance  $\epsilon_{\nu}$  divided by  $\nu$  is given by

$$\omega / \nu =$$

$$C_{a} \sum_{m,n} |\langle \phi_{n}^{r} | \phi_{m}^{p} \rangle|^{2} e^{-G_{s}^{s}(x)/k_{B}T} p_{n}(T) (\mathrm{d}x/\mathrm{d}\nu) / \int_{-\infty}^{\infty} e^{-G_{s}^{s}(x)/k_{B}T} \, \mathrm{d}x$$
(17)

where  $|\langle \phi_n^{\ r} | \phi_m^{\ p} \rangle|^2$  is the Franck-Condon factor for the vibrational modes,  $p_n(T)$  is the equilibrium probability of the solute being in the vibrational state n for the electronic state r,  $C_a$  is given by (9), and  $dx/d\nu$  is obtained from (15) and (16).

For the case where most of the solute molecules are in their zero-point vibrational state for this mode, only the n = 0 terms contribute to the sum in (17), for  $\epsilon_{\nu}$ 's near the absorption maximum. The Franck-Condon factor in (17) then becomes<sup>17</sup>

$$|\langle \phi_0^{\mathsf{r}} | \phi_m^{\mathsf{p}} \rangle|^2 = S^m e^{-S} / \Gamma(m+1), \quad \text{with } S = \lambda_i^{\mathsf{p}} / \hbar \omega_{\mathsf{p}} \tag{18}$$

where  $\Gamma$  is the Gamma function and  $\lambda_{r}^{p}$  is the "vibrational reorganization parameter", computed using the relevant vibrational force constant in the electronic state p. The  $p_0(T)$  in (17) is now

The absorption maximum can be found by finding the largest term in (17) and (18), by maximizing with respect to m and to x. The  $dx/d\nu$  factor is a constant when  $k_p = k_r$ . When  $k_p \neq$  $k_r$  we shall for the present neglect its effect here, but it could be readily considered in an a posteriori calculation. The remaining x-dependent factor has a maximum absorption at x = 0, since  $G_r^s(x)$  is a minimum there. Using Stirling's formula for m! the vibrational Franck-Condon factor appearing in (17) is seen to have a maximum at  $m \simeq S = \lambda_i/\hbar \omega$ . Thereby, from (15) and (16) one finds that the absorption maximum  $\nu_a^{\text{max}}$  occurs at

$$h\nu_{\rm a}^{\rm max} \simeq \lambda_{\rm p} + \lambda_i + \Delta G^0_{\rm rp}$$
 (19)

where  $\lambda_p$  denotes  $1/2k_pa^2$ .

In the absence of the vibrational factor in (16) the absorbance would (again apart from the  $dx/d\nu$  factor) decrease to half its maximum when  $\exp(-k_r x^2/2k_B T)$  equals 1/2, i.e., when  $x = \pm [(2k_B T/k_r) \ln 2]^{1/2}$ . Introducing this x into (15) and (16), the resulting contribution to the full width  $W_a$  of the absorption at half-maximum is found to be

$$W_{\rm a} = 4[\lambda_{\rm p} k_{\rm B} T(k_{\rm p}/k_{\rm r}) \ln 2]^{1/2}$$
 (contribution) (20)

<sup>(15)</sup> An example of this "coordinate" x for dielectrically unsaturated systems is the m + 1/2 introduced in electronic transfer theory in the discussions of solvent fluctuations, in ref 6 and 8.

<sup>(16)</sup> There are really, in the description in ref 5, separate coordinates  $x_1$ and  $x_2$  for the inner-shell solvation for each reactant, so that the right sides of (15) are  $^1/_4k_r(x_1^2+x_2^2)$  and  $^1/_4k_p[(x_1-a)^2+(x_2-a)^2]$ . (Each reactant is taken to have the same solvation "force constant" in a CS reaction.<sup>5</sup>) For the purpose of calculating the widths and the maximum one can show that it suffices, in the case of the CS and CR reactions, to take  $x_1$  and  $x_2$  each equal to some parameter x, as in the present (5). For the CSH (charge-shift) reaction, however, the two parameters  $x_1$  and  $x_2$  are used.

<sup>(17)</sup> E.g.: Ballhausen, C. J. Molecular Electronic Structures of Transition Metal Complexes; McGraw-Hill: New York, 1979; p 112 ff. Curie, D. In Optical Properties of Ions in Solids; NATO Advanced Study Institutes Series, Series B: Physics; Di Bartolo, B., Ed.; Plenum: New York, 1975; Vol. 8, p

An additional contribution to  $W_a$  is found by expansion of the S-dependent factor in (18) as a Gaussian about its maximum at  $S \simeq m$ . It is given by

$$W_{\rm a} \simeq 2[\lambda_i^{\rm p}\hbar\omega_{\rm p}(2 \ln 2)]^{1/2}$$
 (contribution) (21)

This vibrational contribution to the width can be quite large and is frequently dominant. For example, in the usual spectra of aromatic solutes, where the solvent  $\lambda$  (in this case a nonpolar term) is typically minor, there is a dominant high-frequency ring mode progression in the spectrum and the typical value  $^{18}$  of W for spectral transitions between ground and electronic states of neutral aromatic molecules is ~4000 cm<sup>-1</sup>. Roughly similar vibration W's occur for ET reactions and CT spectra (cf. Table II, given

In the model of ref 5a there is a second solvent contribution whose  $\lambda$  will be denoted by  $\lambda_0$  and which arises from the dielectrically unsaturated solvent outside the first shell. Its contribution to  $W_a$  is the usual<sup>1,19</sup>

$$W_a = 4(\lambda_0 k_B T \ln 2)^{1/2} \qquad \text{(contribution)} \tag{22}$$

For a distribution which is Gaussian in the immediate vicinity of the absorption maximum, the square of the full-width  $W_a$  at half-maximum is obtained by adding the squares of all three contributions. We thus have

$$W_{\rm a} \simeq 2[(\lambda_{\rm i}^{\rm p}\hbar\omega_{\rm p} + 2\lambda_{\rm 0}k_{\rm B}T + 2\lambda_{\rm p}k_{\rm B}Tk_{\rm p}/k_{\rm r})(2\ln 2)]^{1/2}$$
 (23)

When the  $\lambda_0$  contribution is also included in (19) for the absorption maximum, the latter can be shown to become

$$h\nu_{\rm a}^{\rm max} = \lambda_{\rm p} + \lambda_{i}^{\rm p} + \lambda_{0} + \Delta G^{0}_{\rm rp} \tag{24}$$

Similarly, for the fluorescence spectrum one finds, as the counterpart of (23) and (24)

$$h\nu_f^{\text{max}} \simeq -\lambda_f - \lambda_i^{\text{r}} - \lambda_0 + \Delta G^0_{\text{rp}}$$
 (25)

and

$$W_{\rm f} \simeq 2[(\lambda_{\rm f}^{\rm r}\hbar\omega_{\rm r} + 2\lambda_{\rm 0}k_{\rm B}T + 2\lambda_{\rm r}k_{\rm B}Tk_{\rm r}/k_{\rm p})(2 \ln 2)]^{1/2}$$
 (26)

There is a minor correction to (24) and (25) when  $\lambda_r \neq \lambda_p$ . The  $\Delta G^0_{rp}$  appearing there does not include the difference of the configurational terms arising from the  $\int \exp(-G^{r}(x)/k_{\rm B}T) \, \mathrm{d}x$  in (17) and from  $\int \exp(-G^p(x)/k_BT) dx$  in the corresponding equation for  $f_\nu/\nu^3$ . More precisely, what is not included is the product in each case of the two such integrals, one per charge center. When this effect is included it can be shown that the true  $\Delta G_{\rm rp}^{0 \, \rm max}$  is given by

$$\Delta G_{\rm rp}^{0 \, \rm max}({\rm true}) = \Delta G_{\rm rp}^{0 \, \rm max} + k_{\rm B} T \ln \left( \lambda_{\rm p} / \lambda_{\rm r} \right) \tag{27}$$

where  $\Delta G^{0}_{rp}^{max}$  is the term appearing in (24) and (25) (cf. (8) of ref 5b)

One further comment on the widths in (23) and (26) concerns the case where the vibrational contribution  $\hbar\omega$  is intermediate rather than relatively large. We consider the case where  $\omega_r$  =  $\omega_{\rm p}$ . The vibrational  $\lambda$ -contribution (denoted now simply by  $\lambda_i$ ) to the width is  $2[\lambda_i \hbar \omega(2 \ln 2)]^{1/2}$ , while if it had been classical it would have been  $2[2\lambda_i k_B T(2 \ln 2)]^{1/2}$ . These two results represent the limiting cases for  $\hbar\omega/2k_{\rm B}T\gg 1$  and  $\hbar\omega/2k_{\rm B}T\ll 1$ , respectively, of the standard expression for the general case, 17 namely,  $2[\lambda_i\hbar\omega[\coth \hbar\omega/2k_BT](2\ln 2)]^{1/2}$ . Finally, in the present model and in that of ref 5a, any nonpolar solvent effect on the widths and on  $\nu_a^{\text{max}}$  and  $\nu_f^{\text{max}}$  is neglected.

#### Widths and Maxima for CS, CR, and CSH Processes

The spectra of many nonpolar aromatics indicate that their value for  $\lambda_i \hbar \omega$  is sufficiently large that it usually constitutes the

TABLE II: Widths of Various CS, CSH, and CR Spectra<sup>a</sup>

system	a/f	type	<i>W</i> , cm <sup>-1</sup>	solvent	ref
HMB-TCPA	a	CS	5000	C <sub>6</sub> H <sub>5</sub> F	23
HMB-TCPA	f	CR	4900	$C_6H_5F$	23
HMB-TCPA	a	CS	5200	DBE	23
HMB-TCPA	f	CR	5800	DBE	23
DBO-TCE	a	CS	~6500	CH₃CN	25
DCMT	a	CS	~4000	hexane	26
DCMT	a	CS	~6400	CH₃CHCl₃	26
DCMT	f	CR	5400	CHCl <sub>3</sub>	26
AAC	a	CS	5500	hexane	26
$DMN-(NB)_2-DCV$	a	CSH	~6500	THF	27
$DMN-(NB)_2-K$	a	CSH	~4700	THF	27
$DMB-(Cn)_2-PMAD$	f	CR	5800	DEE	28
$DMB-(Cn)_2-PMAD$	f	CR	5000	hexane	28
MeOB-Cn-TCP	f	CR	4600	CCl <sub>4</sub>	29
NP-Cn-A	f	CR	4300	$c-C_6H_{12}/C_6H_6$	30
DMABN, etc.	a	LE	~5000	various	31, 32
DMABN, etc.	f	CR	$\sim 5000$	various	31, 32
[2.2]PCQ	a	CS	5800	СН₃ОН	33
[3.3]PCQ	a	CS	5400	dioxane	34, 35
[3.3]MCQ	a	CS	6500	dioxane	35
[2.2.2.2]CQ	a	CS	5500	CH₃OH	36
[3.3]DMMCQ	a	CS	6000	CHCl <sub>3</sub>	37
[2.2]DMMCQ	a	CS	6500	CHCl <sub>3</sub>	38
NaOPC	a	CS	6000	CHCl <sub>3</sub>	40

"The symbols in the first column are defined in the text; a and f denote absorption and fluorescence; LE denotes a locally excited state.

major contribution to the widths W of the absorption and fluorescence bands, a value of  $\sim 4000 \text{ cm}^{-1}$  not being atypical, <sup>18</sup> arising from a progression of a roughly 1000-cm<sup>-1</sup> mode in this spectral transition between ground and excited electronic states of neutral aromatics. Comparable or somewhat larger figures are seen for CT spectra (Table II).

In order to explain some electron-transfer rate constant data in the inverted region, it was postulated in ref 5 that the "force constant" for the solute-inner solvation shell interaction  $k_n$  might be about  $11k_r$ , when the p contains a pair of ions and r a pair of neutrals.  $(k_p = 11k_r \text{ corresponds to } \beta = 0.1 \text{ in Table I.})$  Hence, the corresponding  $\lambda_p$  would be  $11\lambda_r$ . In this case it would follow that the width of the spectral band involving a nonpolar → polar transition in a polar solvent could be very large (cf. Table I for an example for this CS case having  $k_p/k_r = 11$ ).

In Table I we first compare results from (23) and (26) for the widths, namely, (28)-(31) below, with those that can be estimated from existing detailed numerical results of Kakitani and Mataga,<sup>20</sup> who used the partially dielectrically unsaturated model described earlier for  $k^{ET}$ , but with  $\omega_r = \omega_p$ . They considered three types of reaction, as already noted, the charge-separation (CS), charge-recombination (CR), and charge-shift (CSH) reactions. If we let p denote a state containing two ions (+ and -) and r a state containing two neutrals, the present expressions for the absorption and fluorescence widths  $W_a$  and  $W_f$  correspond to the fwhm's which would be obtained for the  $k^{ET}$  vs  $\Delta G^0$  plot for the CS and CR reactions, respectively. They will be denoted by  $W_{CS}$ and  $W_{\rm CR}$ :

$$W_{\rm CS} = 2[(\lambda_{\rm i}^{\rm p}\hbar\omega_{\rm p} + 2\lambda_{\rm 0}k_{\rm B}T + 2\lambda_{\rm p}k_{\rm B}Tk_{\rm p}/k_{\rm r})(2 \ln 2)]^{1/2}$$
 (28)

$$W_{\rm CR} = 2[(\lambda_{\rm r}^{\rm r} \hbar \omega_{\rm r} + 2\lambda_{\rm 0} k_{\rm B} T + 2\lambda_{\rm r} k_{\rm B} T k_{\rm r} / k_{\rm p})(2 \ln 2)]^{1/2}$$
 (29)

where p denotes the polar state and r the nonpolar one.

For the charge-shift reaction (CSH) the width  $W_{\text{CSH}}$  is neither of these, since the charge on one reactant increases and that on the other decreases. In this case the vibrational  $(\lambda_i)$  contribution can be shown to be the mean of those in (23) and (25), i.e.  $^{1}/_{2}(\lambda_{i}^{p}\hbar\omega_{p} + \lambda_{i}^{r}\hbar\omega_{r})$ , with similar remarks applying to the  $\lambda$ 's

<sup>(18)</sup> E.g.: Berlman, I. B. Handbook of Fluorescence Spectra of Aromatic Molecules, 2nd ed.; Academic Press: New York, 1971.
(19) Huang, K.; Rhys, A. Proc. R. Soc. (London) 1950, A204, 406. Lax, M. J. Chem. Phys. 1952, 20, 1752. O'Rourke, R. C. Phys. Rev. 1953, 91, Kubo, R.; Toyozawa, Y. Prog. Theor. Phys. 1955, 13, 160. Markham,
 J. Rev. Mod. Phys. 1959, 31, 956. Kestner, N. R.; Logan, J.; Jortner, J. J. Phys. Chem. 1974, 78, 2148. Ulstrup, J. Charge Transfer Processes in Condensed Media; Springer: New York, 1979.

<sup>(20)</sup> I am indebted to Professor Kakitani for providing a printout of the results from which the data for the widths and positions of the maxima, labeled KM in Table I, could be obtained. The  $\Delta G_{max}^{rp}$  appearing in the last two columns of Table I differs slightly from another quantity  $\Delta G_{rp}^{0}^{max}$  (true) discussed after the present (26).

from the two solvation contributions. (For the CSH calculation we used two x's in the free energy calculation, one per reactant.) We obtained

$$W_{\rm CSH} = (\frac{1}{2}W_{\rm CS}^2 + \frac{1}{2}W_{\rm CR}^2)^{1/2}$$
 (30)

where  $W_{CS}$  and  $W_{CR}$  are given by (28) and (29).

While it is the widths that are of primary interest in the present discussion, more precisely whether a particular  $k^{\rm ET}$  vs  $\Delta G^0$  plot is or is not unexpectedly broad near the maximum  $k^{\rm ET}$ , also important is  $\Delta G^{0 \text{ max}}$ , the value of  $\Delta G^{0}$  where the maximum of the rate constant occurs. The value in ref 5a can be compared with the value predicted from the analogues of (24) and (25):

If p denotes the state with a pair of oppositely charged ions and r denotes that for a pair of neutrals, the  $\Delta G^0$  at which  $k_{\rm rp}^{\rm ET}$  attains its maximum for the CS reaction is given by setting  $h\nu_a^{\rm max}=0$ in (24), since the  $U_r$  and  $U_p$  curves intersect near the minimum of the  $U_{\rm r}$  curve then. Thus,  $\Delta G^{0\,{\rm max}}$  is given by

$$\Delta G^{0}_{CS}^{\text{max}} \equiv \Delta G^{0}_{\text{rp}}^{\text{max}} = -(\lambda_{p} + \lambda_{i}^{p} + \lambda_{0}) \qquad (CS \text{ reaction})$$
(31)

For the CR reaction we find similarly from (25)

$$\Delta G^{0}_{CR}^{max} \equiv \Delta G^{0}_{pr}^{max} = -\Delta G^{0}_{rp}^{max} = -(\lambda_{r} + \lambda_{i}^{r} + \lambda_{0}) \qquad (CR \text{ reaction}) \quad (32)$$

For the CSH reaction, examination of the behavior of each reactant (one x per reactant) shows that  $\Delta G^{0 \text{ max}}$  is the mean of the expressions in (24) and (25):

$$\Delta G^{0}_{\text{CSH}}^{\text{max}} = -\frac{1}{2} (\lambda_{r} + \lambda_{p} + \lambda_{i}^{r} + \lambda_{i}^{p} + 2\lambda_{0})$$
 (33)

where r and p again refer to the nonpolar and polar states, respectively. A comparison of (31)-(33) with detailed numerous results,20 labeled KM, is given in Table I.

It is seen from Table I that the widths are quite well predicted by the simple (28)–(30), and so the latter are useful for analyzing the experimental widths for charge-transfer spectra (and for thermal electron transfer reactions) and so for testing the partial saturation hypothesis of ref 5. The positions of the maxima are also located well enough for (31)-(33) to be useful. The result for  $\Delta G^{0 \text{ max}}$  at  $\beta = 0.1$  is more accurate for the CR reaction than for the CSH and CS reactions. This result is not unexpected, since the high curvature of the  $G^r$  surface for this reaction type serves to localize more sharply the range of the x-coordinate (namely, the vicinity of the minimum of  $G^{r}$ ) that contributes to the  $k^{ET}_{max}$ . This restriction favors the simple approximation used for obtaining (32), namely, that the maximum for a CR reaction occurs at the x = 0 in (15). (For a CS reaction the corresponding approximation used for obtaining (31) is that the maximum occurs at the x = a in (15). In the CSH reaction, where one needs two such coordinates, the maximum occurs at the equivalent of x =0 for one reactant and at x = a for the other.)

Before proceeding with the application of (28)-(33) to data on CT spectra, we consider one final topic, which is rather separate from the above, namely, the determination of  $\Delta G^0_{rp}$  and  $\Delta E_{0\rightarrow 0}$ from absorption/fluorescence spectra.

## 

When both absorption and fluorescence spectra are available, one can determine  $\Delta G^0_{rp}$ , exactly in the case of mirror-image spectra and approximately otherwise. Equations 24 and 25 show that when the  $\lambda$ 's are approximately the same in the two electronic states,  $\Delta G^{0}_{rp}$  is given by

$$\Delta G^{0}_{rp} \simeq (h/2)(\nu_{a}^{max} + \nu_{f}^{max})$$
 (equal  $\lambda$ 's) (34)

Further,  $\lambda$  can be determined from the Stokes shift: The latter,  $h\nu_a^{\text{max}} - h\nu_f^{\text{max}}$ , is seen from (24) and (25) to equal

$$h(\nu_a^{\text{max}} - \nu_f^{\text{max}}) = 2\lambda \quad \text{(equal } \lambda \text{'s)}$$
 (35)

where  $\lambda = \lambda_r + \lambda_i + \lambda_0$ .  $\Delta G^0_{rp}$  is the free energy counterpart of the  $0 \to 0$  transition energy  $\Delta E_{0\to 0}$ , which was written in  $\Delta E^0_{rp}$  in (8): When the motions are all classical, the mean thermal energy in the r state equals that in the p state and so the two cancel in  $\Delta G^0_{\rm rp}$ . Thus,  $\Delta G^0_{\rm rp}$  contains a  $^1/_2k_{\rm B}T \rightarrow ^1/_2k_{\rm B}T$  contribution (i.e., no net contribution) for each classical square term in the Hamiltonian. When, instead, one or more of the motions has a high vibration frequency, that vibration is largely unexcited both in the thermally equilibrated r state and in the thermally equilibrated p state, and so  $\Delta G^0_{rp}$  contains essentially only a  $0 \rightarrow 0$  thermal energy contribution for that vibration. This free energy counterpart,  $\Delta G^0_{rp}$ , of the  $0 \rightarrow 0$  transition energy  $\Delta E_{0\rightarrow 0}$  can be determined from  $h\nu_a^{\text{max}}$  and  $h\nu_f^{\text{max}}$  not only in the case of equal  $\lambda$ 's [(34)] but also when the  $\lambda$ 's in the r and p states are not equal, provided some additional information is available: From (24) and (25) we have a generalization of (34), to unequal  $\lambda$ 's

$$\Delta G_{rp}^{0} = \frac{1}{2}h(\nu_{a}^{\text{max}} + \nu_{f}^{\text{max}}) - \frac{1}{2}(\lambda_{p} - \lambda_{r} + \lambda_{i}^{p} - \lambda_{i}^{r})$$
 (36)

while the Stokes shift  $h(\nu_a^{\text{max}} - \nu_f^{\text{max}})$  is given by

$$h(\nu_{\rm a}^{\rm max} - \nu_{\rm f}^{\rm max}) = \lambda_{\rm r} + \lambda_{\rm p} + \lambda_{i}^{\rm r} + \lambda_{i}^{\rm p} + 2\lambda_{0}$$
 (37)

Thus, if  $\lambda_p/\lambda_r$  and  $\lambda_i^p/\lambda_i^r$  are known and if either  $\lambda_r$  or  $\lambda_i^r$  is known or if one of them is negligible,  $\Delta G^0_{\rm rp}$  can be determined from (36) and (37).  $\Delta S^0_{\rm rp}$  can be determined from  $-\partial \Delta G^0_{\rm rp}/\partial T$ . In this way the  $0 \rightarrow 0$  transition energy  $\Delta E_{0 \rightarrow 0}$  can be obtained:<sup>21</sup>

$$\Delta E_{0\to 0} = \Delta G^{0}_{\rm rp} + T \Delta S^{0}_{\rm rp} \tag{38}$$

The correction to  $\Delta G^0_{\rm rp}$  given in (27) need not be applied here, since it cancels in  $\Delta G^0_{\rm rp}$  and  $T\Delta S^0_{\rm rp}$ .

#### **Experimental Data on Charge-Transfer Spectra**

We next examine some charge-transfer spectra, to see if there are some with the very large widths predicted in ref 5a in their explanation of the apparent absence of an inverted effect for the CS reaction (cf. the present Table I). In this article we shall give some examples rather than attempt to make a comprehensive survey. Some examples of spectral widths include those of pyrazine  $(\sim 4000~\text{cm}^{-1})^{22a}$  and coumarin 153  $(\sim 3500~\text{cm}^{-1})^{.22b}$  Neither of these is particular large, but only small changes of dipole moments of the solute in the r and p states are involved, and, further, there may be additional complicating effects of solvent in the coumarin case.<sup>22b</sup> Other systems are, however, available:

An early example of the study of a charge transfer complex is that of HMB-TCPA (hexamethylbenzene-tetrachlorophthalic anhydride, depicted in Figure 2) for which the ground state is largely neutral and the excited state is largely polar.<sup>23</sup> The absorption here provides the analogue of the CS reaction,<sup>24</sup> and the fluorescence is that of a CR process. The dipole moment of the excited state estimated from the solvent spectra shift was about 15 D.23 Here, in a nonpolar solvent half the Stokes shift, which is the value of  $\lambda$ , was about 3500 cm<sup>-1</sup>. Using this  $\lambda$  and (21), the corresponding contribution (assumed to be vibrational) to the spectral width is predicted to be about 4200 cm<sup>-1</sup>, when  $\hbar\omega \simeq$ 1000 cm<sup>-1</sup>. The total width of the experimental plot, as indicated in the rough plots given in ref 23, is about 5300 cm<sup>-1</sup>. The change in the Stokes shift with polarity of the solvent was appreciable, 23 but the spectral plots themselves are not sufficiently complete or detailed to permit a detailed analysis of the widths. However, examples for two of the solvents used, fluorobenzene and dibutyl ether, are given in Table II. The mirror-image rule is approximately obeyed. Had there been a major difference in the CS and CR widths, there would have been a major exception to the "mirror-image" rule. (A caveat concerning the behavior of CS

The dipole moment estimated in this work from the electric field fluorescence method was somewhat smaller, about 10 D.

<sup>(21)</sup> The difference of  $\Delta H^0_{\rm rp}$  and  $\Delta E^0_{\rm rp}$  is negligible in condensed phases and, indeed, has been neglected throughout. Alternatively, the argument leading from (7)-(14) could have been based on isobaric rather than constant volume ensembles.

<sup>(22) (</sup>a) Baba, H.; Goodman, L.; Valenti, P. C. J. Am. Chem. Soc. 1966, 88, 5410. (b) Maroncelli, M.; Fleming, G. R. J. Chem. Phys. 1987, 86, 6221. (23) Czekalla, J.; Meyer, K.-O. Z. Phys. Chem. (Munich) 1961, 27, 185.

<sup>(24)</sup> A comparison with the light absorption of HMB and of TCPA individually in the CT absorption region (e.g., Cauquis, G.; Basselier, J.-J. Ann. Chim. (Ser. 7) 1962, 746, who give data at -180 °C) reveals that the absorption of the complex is indeed CT rather than that of a locally excited state. I am also indebted to Dr. S. Farid for similar data at room temperature.

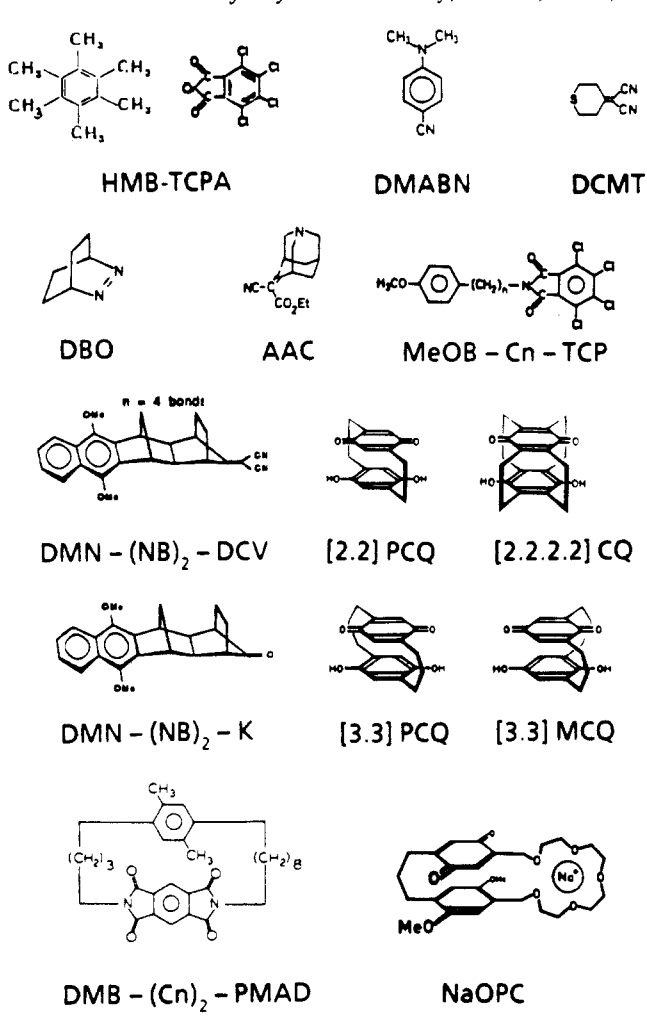


Figure 2. Molecular structures of most of the compounds whose spectral widths are given in Table II.

processes leading to "contact ion pairs" vs those leading to "solvent separated pairs" is discussed in the next section.)

Another interesting example of a charge-transfer complex where absorption of light results in the conversion of neutrals to radical ions (i.e., a CS process) is that between tetracyanoethylene (TCE) and various donors.<sup>25</sup> With diazabicyclooctene (DBO, Figure 2) as donor the value of  $W_a$  is roughly estimated from the plot in ref 25 to be about 6500 cm<sup>-1</sup> (Table II). In the absence of fluorescence information the Stokes shift and hence the reorganization parameter is not known, so as to permit comparison with this value of  $W_a$ . The ions here are probably contact ion pairs.

Other systems with CT absorption spectra of the CS type include dicyanomethylidenethiane (DCMT, Figure 2).26 For hexane and for 1,2-dichloroethane as solvents the widths of this CS system were  $\sim 4000$  and  $\sim 6400$  cm<sup>-1</sup>, respectively (Table II), while the CT fluorescence spectrum in chloroform as solvent had a width of 5400 cm<sup>-1</sup>. The absorption spectrum of azaadamantylidenecyanoacetic acid ethyl ester (AAC, Figure 2) was also determined.26 A plot of this CS spectrum was reported only for hexane as solvent, <sup>26</sup> the width being about 5500 cm<sup>-1</sup> (Table II). Values for polar solvents would be of particular interest.

Examples of charge transfer absorption spectra of the charge-shift (CSH) type include a (dimethoxynaphthalenyl)-(dicyanovinylidene) fused norbornane molecule (DMN-(NB)<sub>2</sub>-DCV, Figure 2) and the corresponding keto compound (DMN-(NB)<sub>2</sub>-K, Figure 2),<sup>27</sup> where the (NB)<sub>2</sub> denotes "fused" norbornanes. The results for the widths are  $\sim 6500$  and  $\sim 4700$  cm<sup>-1</sup>, respectively, when THF is used as the solvent<sup>27</sup> (Table II).

A fluorescent charge transfer spectrum of the CR type is that of a dimethylphenylenepyromellitic acid dimide cyclophane (DMB-(Cn)<sub>2</sub>-PMAD, Figure 2).<sup>28</sup> With diethyl ether as solvent the width was 5800 cm<sup>-1</sup>, while in hexane it was 5000 cm<sup>-1</sup> (Table II).28 The ions here may be, in effect, solvent-separated pairs.

Another system studied was an N-[(methoxyphenyl)propyl]tetrachlorophthalimide (MeOB-Cn-TCP, Figure 2).<sup>29</sup> fluorescence spectrum was of the CR type and had a width of about 4600 cm<sup>-1</sup> in CCl<sub>4</sub>.<sup>29</sup> Also studied was the fluorescence of N-(p-nitrophenyl alkyl)aniline (NP-Cn-A), in cyclohexanebenzene as a solvent,30 the width being about 4300 cm<sup>-1</sup> (Table

There have also been numerous studies of a class of organic molecules, such as (dimethylamino)benzonitrile (DAMBN, Figure 2), which are largely nonpolar in their ground state and have a large dipole moment in the excited state.<sup>26</sup> At first glance they would seem to be ideal as a spectral analogue to the CS reaction, and a large body of work on solvent-shift plots of  $\nu_a - \nu_f$  has assumed, in an estimation of the dipole moment of the excited state, that this fluorescence involves a CS process. However, the light absorption by the nonpolar ground state in many systems of this type appears to first result in a nonpolar excited state ("locally excited state, LE), followed by a subsequent intramolecular electron transfer step between a substituent and the aromatic ring, thereby forming the polar excited state.31,32 Accordingly, the pertinent absorption data do not correspond to a process of the CS type.

A dual fluorescence in those systems occurs from both the polar and the nonpolar states.<sup>32</sup> The W's for the nonpolar  $\rightarrow$  nonpolar absorption and for the polar → nonpolar fluorescence are comparable in these systems, both being apparently dominated by the vibrational contribution of the aromatic ring(s) involved. The width in these systems (Table II) is typically about 5000 cm<sup>-1</sup> judging from the limited data plotted in ref 31a.

The spectra for the nonpolar → nonpolar absorption in a few examples plotted in ref 31 also show some dependence on the solvent. However, even though the initial solute state is nonpolar, the nonnegligible variation of the widths with solvent (e.g., perhaps a 700-cm<sup>-1</sup> difference for the case of benzene and acetone as solvents, as in Figure 2 of ref 31a) indicates that not too much can be read into details of small changes in width of these nonpolar → nonpolar and nonpolar → polar transitions, perhaps because of other solvent effects.

An extensively investigated series of compounds displaying CT absorption spectra (and sometimes the fluorescence was also studied) is that of the various cyclophane quinhydrones, 33-36 their methoxy counterparts, 37,38 derivatives where the quinone has been replaced by tetracyanobenzene as acceptor unit, 39 and compounds such as a cation-bound oligooxaparacyclophane (NaOPC, Figure 2).<sup>40</sup> In Table II, the  $W_a$ 's of particular [2.2]- and [3.3] para-

<sup>(25)</sup> Blackstock, S. C.; Kochi, J. K. J. Am. Chem. Soc. 1987, 109, 2484. (26) Pasman, P.; Rob, F.; Verheoven, J. W. J. Am. Chem. Soc. 1982, 104, 5127.

<sup>(27)</sup> Penfield, K. W.; Miller, J. R.; Paddon-Row, M. N.; Cotsaris, E.; Oliver, A. M.; Hush, N. S. J. Am. Chem. Soc. 1987, 109, 5061.

<sup>(28)</sup> Borkent, J. H.; Verhoeven, J. W.; De Boer, Th. J. Chem. Phys. Lett. 1976, 42, 50.

<sup>(29)</sup> Borkent, J. H.; Verhoeven, J. W.; De Boer, Th. J. Tetrahedron Lett. 1972, 32, 3363.

<sup>(30)</sup> Mutai, K. Chem. Commun. 1970, 1209.

<sup>(31) (</sup>a) E.g.: Lippert, E. Z. Elektrochem. 1957, 61, 962. (b) Lippert, E.; Lüder, W.; Boos, H. In Advances in Molecular Spectroscopy; Mangini, A., Ed.; Macmillan: New York, 1962; Vol. 1, p 443.

<sup>(32)</sup> The dual fluorescence was shown in ref 18. A review of the present situation is given in: Rettig, W. Angew. Chem., Int. Ed. Engl. 1986, 25, 971. Grabowski, Z. R.; Rotkiewicz, K.; Semiarczuk, A.; Cowley, D. J.; Baumann, W. Nouv. J. Chim. 1979, 3, 443. Gilabert, E.; Lapouyade, R.; Rullière, C. Chem. Phys. Lett. 1988, 145, 262

<sup>(33)</sup> Staab, H. A.; Rebafka, W. Chem. Ber. 1977, 110, 3333.
(34) Staab, H. A.; Herz, C. P. Angew. Chem., Int. Ed. Engl. 1977, 16, 799.
(35) Staab, H. A.; Herz, C. P.; Döhling, A.; Krieger, C. Chem. Ber. 1980, 113, 241. The greater width of the MCQ compound, compared with the PCQ, may reflect the greater overlap with a higher frequency absorption band in the MCQ case.

<sup>(36)</sup> Staab, H. A.; Schwendemann, V. M. Liebigs Ann. Chem. 1979, 1258.

<sup>(37)</sup> Staab, H. A.; Döhling, A. Tetrahedron Lett. 1979, 20, 2019.
(38) Staab, H. A.; Reibel, W. R. K.; Krieger, C. Chem. Ber. 1985, 118,

<sup>1230.</sup> 

<sup>(39)</sup> Staab, H. A.; Krieger, C.; Wahl, P.; Kay, K.-Y. Chem. Ber. 1987, 120, 551.

cyclophane quinhydrones ([2.2]- and [3.3]PCQ, Figure 2)<sup>33,34</sup> are given together with those of a [3.3]meta isomer ([3.3]MCQ, Figure 2),35 dimethoxy derivatives ([3.3]DMMCQ, [2.2]-DMMCQ),<sup>37,38</sup> and a [2.2.2.2]cyclophane quinhydrone ([2.2.2.2]CQ, Figure 2),<sup>36</sup> among others.

The average  $W_a$  for their CT spectrum (CS type) of these compounds is seen from Table II to be about 6000 cm<sup>-1</sup>. Fluorescence studies have also been reported, 40,41 and from the value of  $\nu_a - \nu_f$  in a nonpolar solvent a value of  $\lambda_i$  of about 4400 cm<sup>-1</sup> can be estimated for the [2.2] paracyclophane with tetracyanobenzene as acceptor and dimethoxybenzene as donor<sup>40</sup> and a similar value with a dicyanobenzene as acceptor and dimethoxybenzene as donor in a [2.2]metacyclophane.41 A value of about 15 D was determined for the change of dipole moment on excitation, using solvent spectral shift data. In the absence of fluorescence plots it is not possible to conclude from the data presented whether the mirror-image rule is obeyed for these CS-CR processes.

Values of  $\lambda_i$  have been estimated for other systems from the Stokes shift in nonpolar solvents, or from the  $\nu_a$ . For example, a value of about 0.55 eV (~4400 cm<sup>-1</sup>) was estimated<sup>27,42</sup> from such data for the DMN-(NB)2-DCV system in Table II and Figure 2. However, in the case of the keto compound an abnormally small value (0.02 eV) of  $\lambda_i$  was estimated<sup>27</sup> from the  $\nu_a$ . It is best, when possible, to use  $\nu_a - \nu_f$  data, rather than  $\nu_a$ alone, for estimating  $\lambda$ 's. One exception is in the case where the two redox centers are identical, apart from one having the extra electron which is transferred in the optical absorption. In this case  $\nu_a$  provides directly the value of  $\lambda$  (and, in the case of a nonpolar solvent, the value of  $\lambda_i$  when no nonpolar solvent contribution occurs).

In these examples, we have seen (Table II) no evidence as yet that the CS or CSH processes have very large widths as compared to CR processes. On the other hand, the CS process for HMB-TCPA and for DBO-TCE may form contact ion pairs, as noted earlier, whereas Kakitani and Mataga had in mind a dielectric saturation for solvent-separated ion pairs.<sup>43</sup> There is some difference in  $k^{\text{ET}}$ 's for CR reactions involving contact ion pairs and those involving solvent-separated pairs.<sup>43,44</sup> We return to this result in the next section.

The DCMT, AAC, DMN-(NB)<sub>2</sub>-DCV, and DMN-(NB)<sub>2</sub>-K cases in Table II and Figure 2 might correspond to "groupseparated" reactive centers. However, as yet they show no abnormal widths. It would be useful to study CT bands which form in CS processes solvent-separated and reactant-contact ion pairs, to see whether the corresponding CS spectra do show any significant difference of widths. Cyclophanes of different types connecting quinhydrone or other systems might differ one possibility, though the expected decrease in intensity of the CT absorption band when the donor and acceptor become solvent separated may make the measurement of the width W more difficult, unless the CT band is well-separated from the others.

We have seen from the above data and Table II no evidence thus far for abnormal spectral widths, proposed for dielectricsaturated cases,<sup>5</sup> for the CS systems described in Table II. For example, there are no widths close to the value of 14 500 cm<sup>-1</sup> in Table I for  $\beta = 0.1$  nor to the  $10\,000$ -cm<sup>-1</sup> value for  $\beta = 0.3$ (obtained for the  $\lambda$ 's given there). Nevertheless, any conclusion from this finding should be qualified: If the charge separation results in a charge-transfer state strongly admixed with a nonpolar "locally excited" (LE) state, the separated charges are reduced in magnitude ("diluted") and any tendency to dielectric saturation would also be correspondingly reduced.45

Any tendency to a local dielectric saturation depends on both the local charge and the "effective radius" for that charge. These effective radii would appear to be rather small for a molecule such as DCMT in Figure 2, and so would favor dielectric saturation, should it occur. An upper limit to the "dilution" of the separated charges in the CS state is obtained by supposing that all of the absorption intensity to form the CT state comes from borrowing<sup>26</sup> from the oscillator strength of the LE state. (Some of the oscillator strength will come from the pure CT state itself.) On this basis, the fractional charge in the CT state will be approximately equal to or greater than  $(\epsilon_{LE}/\nu_{LE})/[(\epsilon_{CT}/\nu_{CT}) + (\epsilon_{LE}/\nu_{LE})]$ , where we have used (7) and (9). Estimated from the data in ref 26, this ratio is about 0.65, and so the fraction of charge on each of the two centers is at least this amount. Some other systemsintramolecular exciplex systems—involve a fraction between 0.6 and 0.9 of a full charge transfer, as determined from the electric field effect on the fluorescent intensity.46

#### Ion-Pair Recombination

Two methods of forming ion pairs are (1) via a bimolecular quenching of an excited donor (acceptor) molecule by an acceptor (donor) and (2) via a direct excitation within a charge-transfer band. The methods are believed to form, respectively, solventseparated and contact ion pairs.<sup>43,44</sup> For a given  $\Delta G^0$  somewhat different  $k^{\rm ET}$ 's were obtained, the ratio depending on  $\Delta G^{0.43,44}$ 

The results by Farid and co-workers in ref 44 were obtained in the inverted region and showed a crossing of the two log  $k^{ET}$ vs  $-\Delta G^0$  plots. These data were fitted to a dielectrically unsaturated model. The  $-\Delta G^{0 \text{ max}}$  obtained from the fitting was larger, and  $k^{ET,max}$  was smaller, for the "solvent-separated pair" than for the "contact pair". The data, as the authors<sup>44</sup> pointed out, were consistent with the dielectrically unsaturated model,6 since the larger separation distance for the solvent-separated case implies<sup>6</sup> theoretically a larger  $\lambda$  and hence a larger  $-\Delta G^{0 \text{ max}}$ . The predictions of a dielectrically saturated model<sup>5</sup> will instead depend on what values of the various parameters are introduced (e.g., for  $\lambda_p$ , for  $\beta$ , and for the free energy of the (assumed) saturated dielectrically charged system).

The values estimated in ref 44 for  $-\Delta G^{0 \text{ max}}$  for the two types of ion pairs were based on a fitting of the data obtained only in the inverted region, and accordingly, the numerical estimates there are somewhat uncertain. The fitting is such that had parameters leading to a larger  $-\Delta G^{0 \text{ max}}$  been used in the fit, the predicted k<sup>ET,max</sup> would probably have been smaller, as one can see from the nature of the plot there.  $-\Delta G^{0 \text{ max}}$  and  $k^{\text{ET,max}}$  were for the solvent-separated case about 1.8 eV and  $\sim 2 \times 10^{10}$  s<sup>-1</sup>, respectively. For the contact case, these extrapolated results are subject to a greater uncertainty because there was no curvature of the log  $k^{\rm ET}$  vs  $-\Delta G^0$  plot over the narrower  $\Delta G^0$  range investigated. Here,  $-\Delta G^{0\,\rm max}$  and  $k^{\rm ET,max}$  were about 0.8 eV and  $\sim 10^{13}~{\rm s}^{-1}.^{47}$ The same compounds were used for both series, and the compounds were all of the same type.

An entire log  $k^{\rm ET}$  vs  $-\Delta G^0$  plot has actually been determined recently for the solvent-separated pairs by Mataga and coworkers. For the compounds investigated these authors obtained  $-\Delta G^{0\,\text{max}} \simeq 1.5\,\text{eV}$  and  $k^{\text{ET,max}} \sim 10^{11}\,\text{s}^{-1}$ . These values are rather close to those (1.8 eV,  $2 \times 10^{10}$  s<sup>-1</sup>) inferred in ref 44 by a fit of data in the inverted region. (Since the compounds differ in the two studies the values need not be identical, however.) We recall, too, that had a smaller  $-\Delta G^{0 \text{ max}}$  been used in the fit, the  $k^{\text{ET,max}}$ in ref 44 would probably have been larger. There is, therefore, some additional consistency among the differences in the two sets

<sup>(40)</sup> Bauer, H.; Briaire, J.; Staab, H. A. Angew. Chem., Int. Ed. Engl. 1983, 22, 334.

<sup>(41)</sup> Staab, H. A.; Schanne, L.; Krieger, C.; Taglieber, V. Chem. Ber. 1985, 118, 1204.

<sup>(42)</sup> Oevering, H.; Paddon-Row, M. N.; Heppener, M.; Oliver, A. M.; Cotsaris, E.; Verhoeven, J. W.; Hush, N. S. J. Am. Chem. Soc. 1987, 109,

<sup>(43)</sup> Mataga, N. Private communication. Mataga, N. Photochemical Solar Energy; Norris, J., Ed.; in press. (Lecture, 7th International Conference in Photochemical Conversion and Storage of Solar Energy.)

<sup>(44)</sup> Gould, I. R.; Moody, R.; Farid, S. J. Am. Chem. Soc. 1988, 110,

<sup>(45)</sup> This point has been noted by N. Mataga (private communication).
(46) Baumann, W.; Fröhling, J.-C.; Brittinger, C.; Okada, T.; Mataga, N.

Ber. Bunsen-Ges. Phys. Chem. 1988, 92, 700, and references cited therein. (47) We note that one uncertainty, of course, in any comparison of ΔG<sup>0 max</sup> for the two types of ion pairs is in the uncertain value of the Coulombic contribution to  $\Delta G^0$  for the two cases

<sup>(48)</sup> Mataga, N.; Asahi, T.; Kanda, Y.; Okada, T.; Kakitani, T. Chem. Phys., in press.

of studies. It would be very useful, of course to determine also the entire  $\log k^{\rm ET}$  vs  $-\Delta G^0$  plot for the contact ion pairs. As yet, it appears that this desirable goal has not been attained.

it appears that this desirable goal has not been attained. The smaller value for  $k^{\rm ET,max}$  for the solvent-separated pairs, relative to that for the contact pairs, is expected, as the authors of ref 44 have noted, because of the exponential falloff of  $k^{\rm ET}$  with separation distance r,  $k^{\rm ET} \propto \exp(-\alpha r)$ . With an increased r of perhaps 4 Å for the separated pair<sup>44</sup> and with  $\alpha$  being in the vicinity of 1.1 Å<sup>-1</sup> (e.g., ref 49), more or less,  $k^{\rm ET,max}$  would be less by a factor of about 80 for the solvent-separated pairs, compared with the contact pairs.

#### **Concluding Remarks**

We have considered in this brief survey data on organic systems, since the recent discussions<sup>5</sup> of the possible role of partial saturation effects have concentrated on those systems. There is, of course, an important body of studies of CT spectra of inorganic or metal-organic systems (e.g., ref 2 and 14, and references cited therein). In a study of the intervalence CT band of biferrocene<sup>14b</sup> an extrapolation of the CT band to zero polarity of the sovlent indicate s a nonpolar (perhaps vibrational)  $\lambda$  of roughly 3000 cm<sup>-1</sup> for that system.

Further examination of the widths, and indeed also the shapes, of charge-transfer spectra for nonpolar → polar transitions, particularly in organic systems, will be useful for discussing some of the issues treated in this article. Indeed, it would also be interesting to study CS reactions under conditions free or largely free of diffusion control, either by studying bimolecular fluorescence quenching electron transfers at very short times<sup>50</sup> or by studying these quenching reactions in intramolecular systems, particularly under conditions of weak electronic coupling (small CT-LE state mixing). It will also be useful to compare (A1) and (A2) and/or (A3) and (A4), given here for completeness, with the detailed spectral shapes for suitable absorption/fluorescence data.

Acknowledgment. It is a pleasure to acknowledge the support of this research by the Office of Naval Research, as well as very helpful discussions with N. Mataga, T. Kakitani, and S. Farid.

# Appendix: Spectral Plots for the Dielectrically Unsaturated Case

The relevant expressions for the case when there is no dielectric saturation are (13) and (14). We first consider a common situation, namely, where the frequency of the high-frequency vibration is sufficiently high that absorption occurs only from n = 0 and fluorescence only from m = 0. In that case (13) and (14) become<sup>51</sup>

$$\epsilon_{\nu}/\nu = C_{a}h\sum_{m} \frac{e^{-S}S^{m} \exp[-(m\hbar\omega + \Delta G^{0}_{rp} + \lambda_{0} - h\nu)^{2}/4\lambda_{0}k_{B}T]}{\Gamma(m+1)(4\pi\lambda_{0}k_{B}T)^{1/2}}$$
(A1)

and

$$f_{\nu}/\nu^{3} = C_{l}h\sum_{n} \frac{e^{-S}S^{n} \exp[-(n\hbar\omega + \Delta G^{0}_{rp} + \lambda_{0} + h\nu)^{2}/4\lambda_{0}k_{B}T]}{\Gamma(n+1)(4\pi\lambda_{0}k_{B}T)^{1/2}}$$
(A2)

When, instead, the frequency of this mode is not so high, or when the far wings of the spectral band are being explored, far enough that  $\exp(-\hbar\omega/k_BT)$  is nonnegligible, (A1) and (A2) should be replaced by an expression that involves a summation over the initial n's in (13) and m's in (14). When a new pair of variables (n, l) is introduced (n = n, l = m - n) into (13), one obtains at fixed l a factor F(l):

$$F(l) = \sum_{n} |\langle \phi_n^{r} | \phi_{n+l}^{p} \rangle|^2 [\exp(-n\hbar\omega/k_B T)] (1 - \exp(-\hbar\omega/k_B T))$$
(A3)

This factor F(l) is the standard that appeared in the original Huang-Rhys article on F-center optical absorption at each given frequency 19 and so at a fixed value of l. We have  $^{11,14,19}$ 

$$F(l) = [(\bar{n}+1)/\bar{n}]^{1/2} e^{-S(2\bar{n}+1)} I_l(2S[\bar{n}(\bar{n}+1)]^{1/2}) \quad (A4)$$

where  $I_l(z)$  is the modified Bessel function of order l and of complex argument  $z[(I(z) = i^{-l}J_l(iz))]$ , and  $\bar{n}$  is the mean value of the quantum number n at the temperature T: 14,19

$$\bar{n} = \frac{1}{2} \left[ \coth \left( \hbar \omega / 2k_{\rm B}T \right) - 1 \right] \tag{A5}$$

We now have

$$\epsilon_{\nu}/\nu = C_a h (4\pi\lambda_0 k_B T)^{-1/2} \sum_{l} F(l) \exp[-(l\hbar\omega + \Delta G^0_{rp} + \lambda_0 - h\nu)^2/4\lambda_0 k_B T]$$
(A6)

Similar remarks apply to  $f_{\nu}/\nu^3$ , with l now denoting n-m and with the  $\bar{n}$  in (A3) being replaced by  $\bar{m}$  but still having the same value as  $\bar{n}$ :

$$f_{\nu}/\nu^{3} = C_{\rm f}h(4\pi\lambda_{0}k_{\rm B}T)^{-1/2}\sum_{l}F(l) \exp[-(l\hbar\omega + \Delta G^{0}_{\rm rp} + \lambda_{0} + h\nu)^{2}/4\lambda_{0}k_{\rm B}T]$$
(A7)

More complicated expressions, similar to those derived in ref 5, could be obtained for the partially dielectrically saturated case.

Plots of expressions such as (A1) and (A2) may, like analogous  $k^{\rm ET}$  vs  $-\Delta G^0$  plots in the literature for thermal electron transfer reactions, show some "structure" at room temperature even when none is found or essentially found experimentally. The structure is typically a consequence of using the rather artificial one-quantum mode approximation. The latter has the virtue of providing the desired width for the plot, even when  $\lambda_0$  is relatively small, but it can miss the "filling-in" of the spectral structure that could be provided by other modes. One can avoid this by various devices, if desired, but we omit such details here.

<sup>(49)</sup> Marcus, R. A.; Sutin, N. Biochim. Biophys. Acta 1985, 811, 265.

<sup>(50)</sup> Marcus, R. A.; Siders, P. J. Phys. Chem. 1982, 86, 622.

<sup>(51)</sup> Cf. also ref 27 and references cited therein.